

Available online at www.sciencedirect.com**ScienceDirect**

Energy Procedia 126 (201709) 34–41

Energy

Procediawww.elsevier.com/locate/procedia

72nd Conference of the Italian Thermal Machines Engineering Association, ATI2017, 6-8 September 2017, Lecce, Italy

CFD modelling of the condensation inside a Supersonic Nozzle: implementing customized wet-steam model in commercial codes

Mazzelli Federico^{a*}, Giacomelli Francesco^a, Milazzo Adriano^a

^a University of Florence, Department of Industrial Engineering of Florence (DIEF), via di S. Marta 3, 50139, Firenze, Italy.

Abstract

Non-equilibrium condensation of steam occurs in many jet and turbomachinery devices, such as supersonic nozzles, ejectors and across the last stages of steam turbines. Wet steam models are available in many commercial CFD codes and can represent the metastable behaviour of the flow with reasonable accuracy. Unfortunately, the use of built-in models does not allow freedom in the choice of model parameters and settings. In the present paper, a numerical model for the simulation of wet steam flow has been developed and implemented within a commercial CFD code (ANSYS Fluent) via user defined functions. The scheme is based on a single-fluid approach and solves the transport equation for a homogeneous mixture flow coupled with conservation equations for the number of droplets and liquid mass fraction. The model is compared against a well-known steam nozzle test-case.

© 2017 The Authors. Published by Elsevier Ltd.

Peer-review under responsibility of the scientific committee of the 72nd Conference of the Italian Thermal Machines Engineering Association

Keywords: CFD; steam; non-equilibrium; condensation; steam turbine.

1. Introduction

Non-equilibrium condensation of steam occurs in many jet and turbomachinery devices, such as supersonic nozzles and across low pressure stages of steam turbines. Normal operation of these devices involves flow expansions which leads to states that are well within the saturation dome. In the ideal case of a reversible transformation, the attending condensation process would follow a path of equilibrium states, and no losses occur. In real conditions, the very limited residence time and high cooling rates lead to a substantial departure from the equilibrium process. As the steam rapidly

* Corresponding author. Tel.: +39 055 275840.

E-mail address: federico.mazzelli@unifi.it

expands inside a nozzle or blade vane, thermodynamic equilibrium is not maintained and, at a certain degree of expansion, the vapor state collapses and condensation takes place abruptly as a shock-like disturbance [1]. This is generally called the “condensation shock”. This sudden change of state of aggregation leads to an instantaneous and localized heat release that increase the pressure and temperature and reduce the Mach number [1]. More than this, the condensation shock implies large gradients between the phases that cause irreversibilities. Moreover, downstream the condensation shock, the flow contains a considerable number of tiny liquid droplets (of the order of $10^{19}/\text{dm}^3$, [2]) that can interact in non-trivial ways with shock waves and turbulent structures. A reliable CFD scheme should be able to account for all these effects.

In the past decades, several methods have been devised to simulate wet steam flows, with different levels of complexities and accuracy. The simplest and perhaps most used is the so-called “single-fluid” approach. This is basically a fully Eulerian method that solves the continuity equation for both phases separately, whereas the momentum and energy equations are computed for the average properties of the mixture. In addition, a further transport equation is needed to describe the conservation of the number of droplets in the unit volume. This method is commonly employed by commercial codes (e.g. ANSYS Fluent or CFX) and has been used by several research teams [3] [4] [5].

Although commercial codes dispense from developing complex in-house solvers, the use of wet-steam built-in models generally do not allow much freedom in the change of the physical parameters and settings. This work represents an attempt to overcome this limitation through the development of a customized model within a widely used CFD commercial code (ANSYS Fluent, [6]). This approach has the double benefit to allow great flexibility in the choice of the physical model setting (especially for phase change and phase interaction models) and, at the same time, to exploit the capability of commercial software in terms of selection of algorithms and solver settings. The developed scheme is based on a single-fluid approach (mixture model) and is tested and compared against a well-known steam nozzle test-case and a 2D stationary blade cascade.

Nomenclature

h	latent heat [J kg^{-1}]
J	nucleation rate [$\text{s}^{-1} \text{m}^{-3}$]
k	Boltzmann constant [J K^{-1}]
m	mass [kg]
n	number of droplets per unit mass of mixture [kg^{-1}]
p	pressure [Pa]
R	specific gas constant [$\text{J kg}^{-1} \text{K}^{-1}$]
r	radius [m]
T	temperature [K]
u	velocity [m s^{-1}]

greek letters

α	volume fraction [-]
β	mass fraction [-]
Γ	liquid mass generation rate [$\text{kg m}^{-3} \text{s}^{-1}$]
γ	specific heat ratio [-]
ρ	density [kg m^{-3}]
σ	surface tension [J m^{-2}]
ϕ_{ss}	supersaturation ratio [-]

subscripts

d	droplet
m	mixture, molecule
v	vapour

2. Model Description

The particular set of equations presented in this section represent a common choice in the literature [7], and were considered for this work in order to allow the benchmark of the developed scheme against the Fluent built-in model.

The Single-fluid model is based on a fully Eulerian, homogeneous approach that assumes the liquid phase to be uniformly dispersed within the vapour volume. The conservation equations for mass, momentum and energy are then written based on mixture properties and assume the form of the conventional Navier-Stokes equations for compressible flows:

$\frac{\partial \rho_m}{\partial t} + \frac{\partial \rho_m u_{mj}}{\partial x_j} = 0$ $\frac{\partial \rho_m u_{mi}}{\partial t} + \frac{\partial \rho_m u_{mi} u_{mj}}{\partial x_j} = -\frac{\partial p}{\partial x_j} + \frac{\partial \tau_{ij_eff}}{\partial x_j}$ $\frac{\partial \rho_m E_m}{\partial t} + \frac{\partial \rho_m u_{mi} H_m}{\partial x_j} = \frac{\partial q_{j_eff}}{\partial x_j} + \frac{\partial u_{mi} \tau_{ij_eff}}{\partial x_j}$	(1)
---	-----

In eq. 1 the properties of the mixture are described by means of mass weighted averages in the case of extensive quantities:

$\zeta_m = \beta \zeta_l + (1 - \beta) \zeta_v$ $\omega_m = \alpha_l \omega_l + (1 - \alpha_l) \omega_v$	(2)
--	-----

where ζ_m represents any of the mixture thermodynamic extensive properties (e.g. enthalpy, entropy, total energy, etc...), ω_m is a mixture intensive property (e.g., density, temperature, specific heat capacity), β is the liquid mass fraction and α_l is the liquid volume fraction. The connection between these last two quantities is straightforward:

$\beta = \frac{m_l}{m_l + m_v} = \frac{\alpha_l \rho_l}{\alpha_l \rho_l + (1 - \alpha_l) \rho_v}$	(3)
---	-----

In addition to the transport equation for the mixture, two further equations are needed for the conservation of the liquid mass and the number of liquid droplets:

$\frac{\partial \rho_m n}{\partial t} + \frac{\partial \rho_m u_{mj} n}{\partial x_j} = \alpha_v J$ $\frac{\partial \rho_l \alpha_L}{\partial t} + \frac{\partial \rho_l u_{mj} \alpha_L}{\partial x_j} = \Gamma$	(4)
---	-----

where “n” is the number of droplets per unit mass of the mixture and it is assumed that no slip exists between the phases so that the two phase moves at the same speed.

The term “J” in eq. 4 represents the rate of nucleation of new generated droplets per unit volume of vapour and is expressed here through the classical nucleation theory (more details can be found in [8]) modified with Kantrowitz non-isothermal correction [9]:

$J = \frac{q_c}{(1 + \xi)} \frac{\rho_v^2}{\rho_l} \left(\frac{2\sigma}{\pi m_m^3} \right)^{1/2} \exp \left(-\frac{\Delta G b^*}{k T_v} \right)$	(5)
--	-----

$$\xi = q_c \frac{2(\gamma - 1)}{(\gamma + 1)} \frac{h_{lv}}{RT_v} \left(\frac{h_{lv}}{RT_v} - \frac{1}{2} \right)$$

where ξ is the Kantrowitz non-isothermal correction, q_c is the accommodation factor, h_{lv} is the liquid-vapour latent heat, σ is the liquid water surface tension and ΔGb^* is Gibbs Free energy needed to form a stable liquid cluster (other thermodynamic constants are defined in the nomenclature). Thermodynamic stability considerations lead to a simple expression for the Gibbs free energy of a critical cluster [8]:

$$\Delta Gb^* = \frac{4}{3} \pi r^{*2} \sigma \quad (6)$$

where r^* is the critical radius a stable liquid cluster and φ_{ss} is the supersaturation ratio:

$$r^* = \frac{2\sigma}{\rho_l RT_v \cdot \ln \varphi_{ss}}$$

$$\varphi_{ss} = \frac{P_v}{P_{sat}(T_v)} \quad (7)$$

The Gibbs free energy of a critical cluster represents the energy barrier that must be overcome by the vapor to form a stable liquid cluster. Equations from 5 - 7 gives the rate at which liquid nuclei spontaneously form within the vapor stream. The presence of the exponential in eq. 5 is indicative of the shock-like nature of the condensation phenomenon. Moreover, it is important to note that all the variables of equation 5 - 7 depend solely on the vapor thermodynamic state.

In order to close the set of flow governing equation, it is necessary to provide a law for the liquid mass generation rate per unit volume of mixture, Γ , in eq. 4. This stems from two different sources:

$$\Gamma = \Gamma_{nuc} + \Gamma_{grow} = \alpha_v m_d^* J + \rho_m n \frac{dm_d}{dt} \quad (8)$$

where m_d is the mass of a generic liquid droplet and m_d^* is its value when the liquid nucleus first forms:

$$m_d^* = \frac{4}{3} \pi \rho_l r^{*3}$$

$$m_d = \frac{4}{3} \pi \rho_l r_d^3 = \frac{\rho_l \alpha_l}{\rho_m n} \quad (9)$$

where it is assumed that all liquid droplets have spherical shape.

The first of the two addenda in the RHS of eq. 8 describes the mass generated from freshly nucleated droplets. This term is significant only in the first stages of the condensation process and it gets rapidly overtaken by the second addendum Γ_{grow} , which represents the growth or shrinkage of existing droplets. Its expression requires the definition of a droplet growth law. In this work we use the formulation derived by Hill [2] following a statistical mechanics approach and later rearranged by Young [10]:

$$\frac{dr_d}{dt} = \frac{p_v}{\rho_l h_{lv} \sqrt{2\pi RT_v}} \frac{c_p + c_v}{2} \cdot (T_s(p_v) - T_v) \quad (10)$$

By making use of equations from 1 to 10 form a closed system of equations that can be solved as long as expressions for the vapor and liquid equation of state and thermodynamic properties are provided.

Calculations of the non-equilibrium phase-change of steam necessarily requires the description of the fluid properties in metastable conditions, meaning that common tabulated properties cannot be used to this purpose. Unfortunately, there is a serious lack of experimental data for the properties of steam in supercooled conditions, which is regularly testified by reports of the International Association for the Properties of Water and Steam [11]. Consequently, in order to perform wet steam calculations, it is necessary to extrapolate a generic equation of state outside its normal range of validity to describe metastable states within the saturation curve.

In the present work, the steam properties are calculated following the work of Young [12] who derived a Virial equation of state truncated at the third term of the expansion:

$p = \rho_v RT_v \cdot (1 + B\rho_v + C\rho_v^2)$	(11)
---	------

where B and C are the second and third Virial coefficients. These are function of the sole temperature their expressions were calibrated to match steam data in the range between 273.16 and 1073 K. Moreover, formulations for the enthalpy, entropy and specific heats are derived from the Virial equations based on a procedure described by Young [12]. Moreover, the steam thermal conductivity and dynamic viscosity are given by low order polynomial function of the vapor temperature obtained from interpolation of NIST dataset [13]. Finally, the liquid phase properties (viz., liquid density, specific heat capacity, thermal conductivity and viscosity) are calculated assuming saturation conditions and are again expressed through empirical correlations obtained from NIST [13].

3. Numerical setup

The validation of the presented model is made by comparing the simulation results with the experimental data of the converging-diverging nozzle of Moses and Stein [14]. The results are also confronted with those obtained with the ANSYS Fluent build-in wet steam model in order to benchmark the present scheme with a previously validated code. In this respect, it should be noted that the droplet generation and growth rates equations are the same as those featured by the Fluent build-in model. Future studies will address the analysis of different phase change models.

The set of boundary conditions for the simulations are summarized in Table 1, the experiments considered in the present paper correspond to n. 193 and n. 252 of reference [14] and [7]. Simulations are performed using the commercial CFD package ANSYS Fluent v18.0, which is based on a finite volume approach. In order to set up the model within ANSYS Fluent, it was necessary to rely on the code customization features. Precisely, the model was developed within the framework of Fluent pressure-based multiphase solver by adding a number of User Defined Functions (UDF). Of these, two were needed to input the source terms for the liquid mass fraction and droplet number transport equation. One further UDF was needed to enforce the expression for the diameter of the condensed phase. Finally, a User Defined Real Gas Model was built to implement the virial equation of state and transport properties of the continuous phase.

Figure 1 shows the computational domain used for all the CFD analyses. The grid has approximately 30*000 quadrilateral cells and is designed to have y^+ values always less than 1 along the nozzle surfaces. The size of the grid was selected based on previous studies made on the same geometry with the ANSYS Fluent wet-steam model [15]. The $k-\omega$ SST turbulence model is adopted for all simulations due to the specific calibration for transonic applications [16]. Convergence of the solution is defined by an error in the mass flow imbalance of less than 10^{-5} kg s^{-1} and calculations are stopped when all residuals are stable. Walls are assumed to be adiabatic and smooth.

The solution of the governing equations is achieved through a pressure-based coupled solver for the customized mixture model, whereas the ANSYS Fluent built-in uses a density based solver. In this regard, it should be noted that, within Fluent, the only solvers available to build customized multiphase models are pressure-based. However, the application these types of solvers may be questionable in compressible flows experiencing pressure or condensation shocks. Therefore, in order to limit problems of numerical diffusion, a third order accurate QUICK scheme is selected for the spatial discretization of all transport equations. As will be shown in the next section, the comparison with the

Fluent built-in model compares favourably and demonstrate that problems related to solver scheme should be limited, at least for the high order discretization schemes adopted in this work.

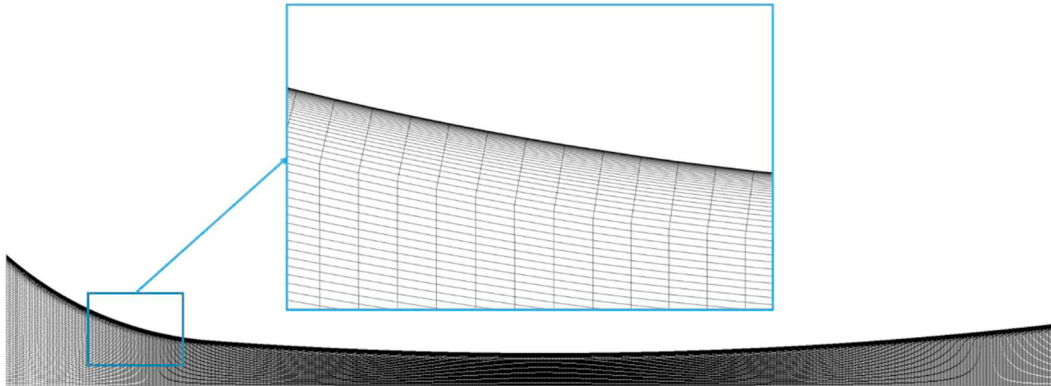


Figure 1 – Computational domain

Table 1: Summary of nozzle boundary conditions

Experiment	Inlet Total Pressure [Pa]	Inlet Total Temperature [K]
N. 193	43023	366
N. 252	40050	374

4. Results

Figure 2 shows a comparison between CFD results and experiments in terms of pressure profile along the nozzle axis for the two different cases simulated. The figure focus on the region downstream the nozzle throat (located at $x=8,22$ mm) where the condensation shock takes place and experimental measurements are available. Clearly, the two CFD schemes overlaps on each other and seem to approximately capture the experimental trend, although some discrepancies exist. In particular, the CFD curves corresponding to the exp. 193 seem to reproduce correctly the steepness of the pressure rise, whereas the location of the condensation shock is somewhat anticipated. Conversely, numerical results for the exp. 252 seem to underestimate the pressure level as well as the steepness of the pressure rise. Nevertheless, the agreement may be considered satisfactory in view of the experimental uncertainty and of the assumption connected to the single-fluid, homogeneous approach.

A further mean to assess the accuracy of wet-steam models is by comparison with data for the average droplet radii within the nozzle. Moses and Stein [14] performed light scattering measurement for the exp. 252 that were processed by Young [10] in order to calculate values of Sauter mean radii along the axis. Figure 3 shows a comparison between these data and the results of the present model. The results show that CFD predicts values for the radii that are approximately a half of the experimental. Nevertheless, it is known that for this case there is a general tendency to under-predict droplet sizes [7]. Moreover, the discrepancy could be partly explained by the different average definition. In the CFD simulations, the droplet radius represents a volume averaged mean, whereas in the experiment the Sauter mean radius is used. The comparison of these two averaged values requires knowledge of the droplets radii distribution in the steam and, in principle, for polydispersed droplets population the volume mean is always less than Sauter [17]. For the distributions measured in the turbine cascades (e.g. [18]) the ratio of volume mean radius to the Sauter radius is about 0.6, which is very close to the difference between the presented results.

Finally, it is interesting to note that the numerical trends for the average radius tend to predict different slope of the curve in the region downstream the condensation shock. In particular, the Fluent built-in model predicts the presence of a plateau towards the exit of the nozzle, whereas the developed model shows an increasing trend more similar to the experimental value.

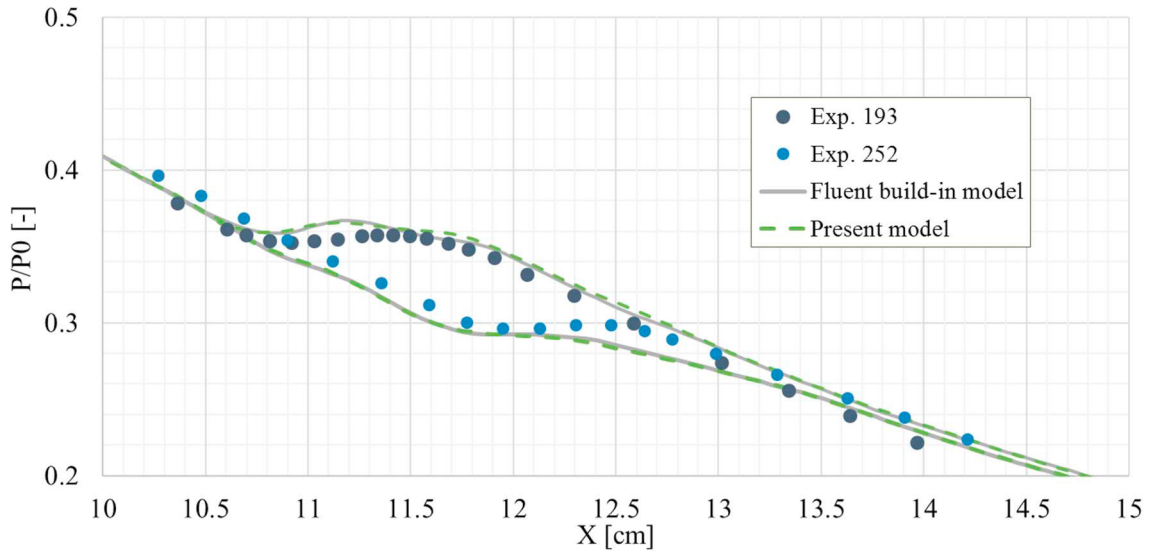


Figure 2– Pressure along the axis

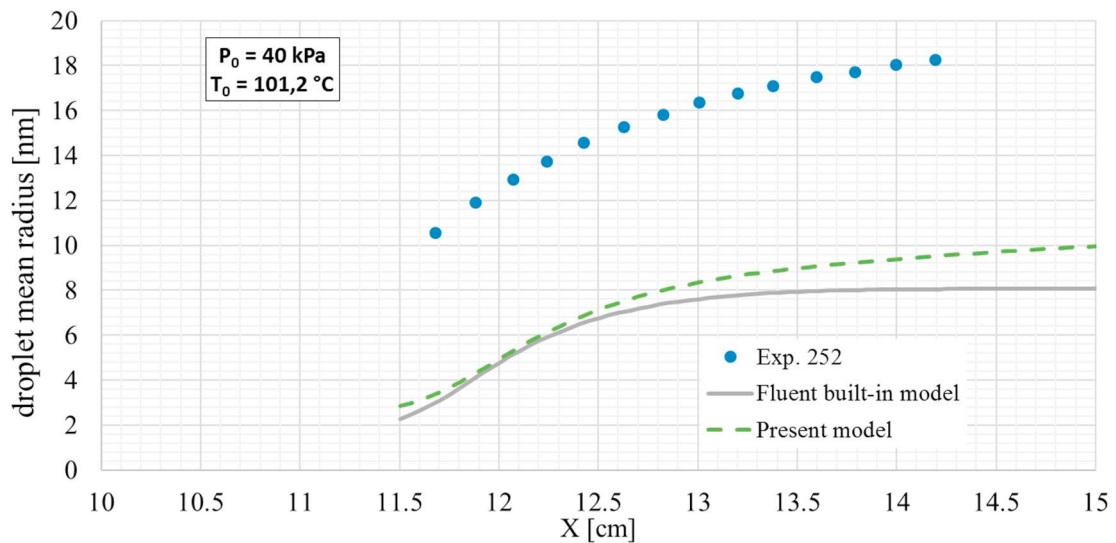


Figure 3– Mean droplet radius along the axis

5. Conclusions

A numerical model for the simulation of wet steam flow has been developed and implemented within a commercial CFD code (ANSYS Fluent) via user defined functions. The scheme is based on a single-fluid approach and solves the transport equation for a homogeneous mixture flow coupled with conservation equations for the number of droplets and liquid mass fraction.

The model has been compared against a well-known steam nozzle test-case. The results are also confronted with those obtained with the ANSYS Fluent build-in wet steam model in order to benchmark the present scheme with a previously validated code.

Results for the pressure profile along the nozzle axis have shown that the present model overlaps the trend of the Fluent built-in model and both give a good agreement with experiments. Conversely, the comparison is somewhat less satisfactory when comparing the results for the droplet average radii. In this regard, discrepancies with experiments are in line with other models in the literature and can be partly explained by the difference in the average definitions.

References

- [1] P. P. Wegener e L. M. Mack, «Condensation in Supersonic Wind Tunnels,» in *Advances in Applied Mechanics*, New York, Academic Press Inc., 1958, pp. 307-440.
- [2] P. G. Hill, «Condensation of water vapour during supersonic expansion in nozzles,» *J. Fluid Mech.*, vol. 25, n. 3, pp. 593-620, 1966.
- [3] K. Ariaifar, D. Buttsworth e G. Al-Doori, «Effecto of mixing on the performance of wet steam ejectors,» *Energy*, vol. 93, pp. 2030-2041, 2015.
- [4] F. Giacomelli, G. Biferi, F. Mazzelli e A. Milazzo, «CFD modeling of supersonic condensation inside a steam ejector,» *Energy Procedia*, n. 101, pp. 1224-1231, 2016.
- [5] F. Mazzelli, D. Brezgin, I. Murmanskii, N. Zhelonkin e A. Milazzo, «Condensation in supersonic steam ejectors: comparison of theoretical and numerical models,» in *Proceedings of 9th International Conference on Multiphase Flow*, Florence, 2016.
- [6] ANSYS Inc., ANSYS Fluent Theory Guide, Canonsburg, PA: release 18.0, 2016.
- [7] J. Starzmann, F. R. Huges, A. J. White, J. Halama, V. Hric, M. Kolovratnik, H. Lee, L. Sova, M. Statny, S. Schuster, M. Grubel, M. Schatz, D. M. Vogt, P. Y., G. Patel, T. Turunen-Saaresti, V. Gribin, V. Tishchenko, I. Garilov e e. al., «Results of the International Wet Steam Modelling Project,» Prague, 2016.
- [8] F. Bakhtar, J. B. Young, A. J. White e D. A. Simpson, «Classical nucleation theory and its application to condensing steam flow calculations,» in *Proceedings of the Institution of Mechanical Engineers, Part C: Journal of Mechanical Engineers Science*, 2005.
- [9] A. Kantrovitz, «Nucleation in very rapid vapour expansions,» *J. Chem. Phys.*, vol. 19, pp. 1097-1100, 1951.
- [10] J. B. Young, «The Spontaneous Condensation in Supersonic Nozzles,» *PhysicoChemical Hydrodynamics*, vol. 3, n. 1, pp. 57-82, 1982.
- [11] International Assotiation for the Properties of Water and Steam, «Thermophysical Properties of Metastable Steam and Homogeneous Nucleation,» 2011.
- [12] J. B. Young, «An Equation of State for Steam for Turbomachinery and Other Flow Calculations,» *Journal of Engineering for Gas Turbines and Power*, vol. 110, n. 1, pp. 1-7, 1988.
- [13] E. Lemmon, M. Huber e M. McLinden, «NIST Standard Reference Database 23: Reference Fluid Thermodynamic and Transport Properties-REFPROP, Version 9.1,» 2013.
- [14] C. A. Moses e G. D. Stein, «On the growth of steam droplets formed in a Laval nozzle using both static pressure and light scattering measurements,» *Journal of Fluids Engineering*, pp. 311-322, 1978.
- [15] F. Giacomelli, F. Mazzelli e A. Milazzo, «CFD modeling of high-speed condensation in supersonic nozzles, part I: steam,» in *Fourth International Conference on Computational Methods for Thermal Problems, ThermaComp*, Atlanta, USA, 2016.
- [16] F. R. Menter, «Two-Equation Eddy-Viscosity Turbulence Models for Engineering Applications,» *AIAA Journal*, vol. 32, n. 8, pp. 1598-1605, 1994.
- [17] W. Wroblewski, S. Dykas e A. Gepert, «Steam condensing flow modeling in turbine channels,» *International Journal of Multiphase Flow*, vol. 35, pp. 498-506, 2009.
- [18] V. Petr e M. Kolovratnik, «Heterogeneous effects in the droplet nucleation process in LP steam turbines,» in *Poceedings of the 4th European Conference on Turbomachinery*, Florence, 2001.